

Biofunctionalization of β -cyclodextrin nanospikes using cholesterol

Parbeen Singh^{a,b}, Xiaohong Ren^a, Tao Guo^a, Li Wu^a, Shailendra Shakya^{a,b}, Yaping He^{a,b}, Caifen Wang^a, Abi Maharjan^{a,b}, Vikramjeet Singh^{a,*}, Jiwen Zhang^{a,b,*}

^a Center for Drug Delivery System, Shanghai Institute of Materia Medica, Chinese Academy of Sciences, Shanghai 201203, China

^b University of Chinese Academy of Sciences, Beijing 100049, China



ARTICLE INFO

Keywords:
Biofunctionalization
 β -CD nanospike
Cholesterol
Cellular uptake

ABSTRACT

Cyclodextrins nanospikes (CD-NSPs) are highly microporous crosslinked polymers with potential applications in the delivery of small and macro-molecular therapeutic agents. Despite the potent host-guest inclusion property, their inherent lack of cellular binding ability has limited applications in drug delivery. Herein, we functionalized the surface of β -cyclodextrin nanospike (β -CD-NSP) with cholesterol, which is endogenous physiological molecules, widely distributed in all cells, and responsible for cell interactions and protein binding. The surface grafting of synthesized β -CD-NSP was confirmed with spectroscopic, microscopic, thermogravimetric, and chromatographic techniques. Moreover, β -CD-NSP was found to be safe in cytotoxicity assay. Doxorubicin (Dox) was selected as a model drug for drug adsorption study of cholesterol hydrogen succinate (CHS) grafted β -CD-NSP. The cellular uptake of NSP was found to be enhanced after CHS modification confirmed by confocal laser scanning microscopy (CLSM). Thus, proposed CHS modified β -CD-NSP system could be used as a site-specific drug delivery carrier.

1. Introduction

Cyclodextrins (CDs) are oligosaccharides consisting of six, seven or eight glucopyranose units connected by 1,4-glycosidic linkage and have capacity to form inclusion complex with both hydrophilic and hydrophobic guest molecules (Szejtli, 1998). The host-guest inclusion complexes of CD-drug have capacity to increase the aqueous solubility of poorly water-soluble drugs, improve the stability, and mask the unacceptable taste of drugs (Crini, 2014; Guo et al., 2017; Loftsson, Brewster, & Måsson, 2004). In modern drug delivery system, CDs are the choice of supramolecular host molecules for preparation of drug carriers in form of micelles, vesicles, hydrogels, metal organic frameworks and nanoparticles (Hartlieb et al., 2016; Ma & Zhao, 2015; Mejia-Ariza, Grana-Suarez, Verboom, & Huskens, 2017; Wang, Liu, Liang, & Zou, 2017; Zhang & Ma, 2013). Free availability of hydroxyl groups makes them suitable for crosslinking with other molecules or between CD molecules. CDs based inter-crosslinked polymers, better known as nanospikes (NSPs) are new class of hyper-reticulated crosslinked polymers that improve the solubility, absorption, bioavailability, and control the release of different drugs (Alongi, Poskovic, Frache, & Trotta, 2010; Ansari, Torne, Vavia, Trotta, & Cavalli, 2011; Gigliotti et al., 2016; Sherje, Dravyakar, Kadam, & Jadhav, 2017; Swaminathan, Cavalli, & Trotta, 2016; Swaminathan et al., 2010; Venuti et al., 2017).

CD-NSPs are advanced crosslinked polymers that are

nanostructured within three-dimensional network. These materials are highly porous and hyper-branched polymers with the ability to instantly attend nanometric dimensions when dispersed in water (Caldera, Tannous, Cavalli, Zanetti, & Trotta, 2017; Chilajwar, Pednekar, Jadhav, Gupta, & Kadam, 2014). The incorporation of drugs within the structure either as inclusion complexes or as non-inclusion is a characteristic feature of NSPs. Interestingly, the encapsulation properties of NSPs could be used to treat specific diseases such as cancer, cardiovascular disorders by direct delivery of the drug into the site of action, but the applications are unfortunately hampered in many cases by their non-binding nature and lack of interactions with specific proteins or cell membranes.

The post/pre-modification of polymers with biomolecules or targeting moiety is widely applied to improve the interaction with cells or receptors (Park et al., 2014; Trotta et al., 2016). Meanwhile, surface modification of drug carriers can alter the cellular uptake and the therapeutic properties of nanocarrier systems. Here, we selected cholesterol (CL), a universal biomolecule that plays various important roles in the mammalian cellular process with both hydrophilic and lipophilic properties for surface functionalization of β -CD-NSP (Ercole, Whittaker, Quinn, & Davis, 2015; Hosta-Rigau, Zhang, Teo, Postma, & Stadler, 2013; Ikonen, 2008). In addition, CL is heterogeneously distributed between the cellular membranes and enriched in the plasma membrane. The interaction of CL with lipids, other membranes, and specific

* Corresponding authors at: Center for Drug Delivery Systems, Shanghai Institute of Materia Medica, Chinese Academy of Sciences, No. 501 of Haik Road, Shanghai 201203, China.
E-mail addresses: singh.simm@outlook.com (V. Singh), jwzhang@simm.ac.cn (J. Zhang).

proteins affects the cellular processes. Moreover, structure and properties of CL enhance the bio-adhesion by a special biophysical mechanism (Murata et al., 1995; Simons & Vaz, 2004). However, some membrane proteins can bind tightly with cholesterol and some proteins are involved in cellular cholesterol homeostasis (Nohturfft, Brown, & Goldstein, 1998). In our previous research, it has been demonstrated that cholesterol modified CD-MOF nanocarrier significantly enhanced the blood plasma concentration of Dox in rats as well as enhanced the cellular uptake (Singh, Guo et al., 2017).

In another report, we described the formation of crystalline and amorphous NSPs from different CDs compounds and their effects on drug loading capacity at different crosslinking ratios (Singh, Xu et al., 2017). Due to intrinsic properties of NSPs to enhance the solubility and bioavailability of guest molecules as a drug carrier and cellular binding and protein interaction properties of CHS as a biomolecule, it is worthy to try the effect of CHS grafting on NSP particles. The intensive research has been published on the synthesis, drug absorption, solubility, and bioavailability enhancement so far but not a single research has been reported for biofunctionalization of CD-NSP to our knowledge. In this research, we developed a straightforward one-step effective strategy to graft the CHS in order to enhance the cellular binding efficiency of β -CD-NSP. CHS content in the β -CD-NSP was quantified by liquid chromatography after hydrolysis by ammonia. For the proof of concept, one of the most widely used anticancer drug Dox was selected as a model drug. The changes in the physicochemical and biological aspect of β -CD-NSP after grafting with CHS and future directions are discussed in this report.

2. Experimental section

2.1. Materials

β -cyclodextrin (β -CD) was purchased from Anhui Sunhere Pharmaceutical Excipients Co., Ltd (China). Diphenyl carbonate (DPC, > 99.0% purity) was purchased from Shanghai Aladdin Bio-Chem Technology Co., Ltd (China). Triethylamine (TEA, 99.0% purity), dimethylformamide (DMF, 99.5% purity), ethanol (EtOH > 99.0% purity), 1-ethyl-3-(3-dimethyl aminopropyl) carbodiimide (EDC, 99.0% purity), 4-dimethylamino pyridine (DMAP, 99.0% purity), all other chemicals and reagents used were of analytical grade, purchased from Sinopharm Chemical Reagent Co., Ltd., (China) and used without further purification. Cholesterol hydrogen succinate (CHS, > 97.0% purity) was purchased from Tokyo chemical industry Co., Ltd (Japan). Doxorubicin (> 99.5% purity) was purchased from Dalian Meilun Biotech Co., Ltd. (Dalian, China). HeLa cells were obtained from Chinese Academy of Sciences (Shanghai, China). Dulbecco's modified eagle's medium (DMEM) and fetal bovine serum (FBS) were purchased from Gibco Thermo Fisher Scientific Ltd (USA). Cell labeling dye DAPI H-1200 was purchased from Vector Laboratories Inc., USA.

2.2. Synthesis of β -CD-NSP

The β -CD-NSP was synthesized according to the previously reported method from our lab (Singh, Xu et al., 2017). Briefly, 60 mM solution of β -CD (0.681 g) in 10 mL DMF was prepared in round bottom flask and heated up to 80 °C to obtain a clear solution with 400 rpm stirring rate. Subsequently, DPC (0.514 g, 240 mM) was added to a molar ratio of 1:4. To reduce the reaction time, TEA (350 μ L) was used as catalyst and reaction was carried out for 12 h. Once the reaction was completed, the crude was poured into water, and centrifuged at 4500 rpm for 10 mins. The residue was re-suspended into purified water, mechanically disaggregated by vortex, and again centrifuged. The precipitate was washed by the slurry in ethanol (Soxhlet extraction, 8 h) and distilled water to remove the unreacted reagents and by-products particularly phenol. The obtained NSP samples were freezed at -78 °C for 4 h and then lyophilized overnight to keep their original intact structure. After

drying, obtained sample was weighed which produced 71% yield.

2.3. CHS grafting onto the surface of β -CD-NSP

The β -CD-NSP was functionalized with CHS as per previously reported methods with slight modification (Shen, Li, & Yang, 2014; Singh, Guo et al., 2017). Briefly, 145 mg of CHS was activated by 86 mg of EDC (1.5 mol equivalent to CHS) and 54 mg of DMAP (1 mol equivalent to CHS) in 30 mL of dry DMF and 1.0 g β -CD-NSP was added. The reaction mass was continuously stirred at 45 °C for 24 h. After completion of the reaction, the crude mass was cooled down to room temperature and precipitated mass was extensively washed with ethanol and water to remove unreacted reagents including unreacted CHS. Furthermore, the crude material was dried under same conditions as for NSP to harvest the β -CD-NSP-CHS which produced 83% yield.

2.4. Characterization

2.4.1. FTIR characterization

The prepared samples of β -CD-NSP and β -CD-NSP-CHS were characterized by synchrotron radiation Fourier-transform infrared spectroscopy (SR-FTIR). SR-FTIR spectroscopy was performed for chemical confirmation by BL01B beamline at Shanghai Synchrotron Radiation Facility (Shanghai, China). FTIR spectra of all samples were recorded by using synchrotron radiation based Thermo-scientific system Nicolet™iS™5 FT-IR spectrophotometer in the region of 4000–650 cm^{-1} . All the data were further processed by OMNIC software.

2.4.2. Water contact angle and swelling study

To check the CHS effect on the surface of NSP after grafting, water contact angle of modified NSP was determined. The samples of NSP and CHS grafted NSP were compressed to form a tablet with a flat surface. Then, a water drop was placed onto the surface of samples and the contact angle was captured with the digital camera. Further, images were processed with Image Pro software and water contact angle measured.

Swelling study of surface samples was carried out in distilled water as swelling solutions. The weighed amounts of dried samples were dissolved with swelling solution at room temperature in mechanical shaker at 75 rpm. After 20 mins, the samples were separated from the swelling solution and wiped out with filter paper and weighed. Swelling ratio (S_t) of samples were calculated according to Eq. (1)

$$S_t = (w_1 - w_2)/w_2 \quad (1)$$

where, w_1 was the weight of the samples in swollen state and w_2 was the initial weight of samples.

2.4.3. Particle size and zeta potential measurement

After washing, all the samples were evaluated for size distribution and zeta potential using water as the dispersion medium. The dynamic light scattering related measurements were carried out on Malvern Zetasizer, Nano series (Nano ZS90, UK). All the samples were measured in triplicates.

2.4.4. Thermal characterization by DSC and TGA

Differential scanning calorimetry (DSC) analysis was performed with differential scanning calorimeter (Mettler Toledo ST, Switzerland) equipped with intracooler to get additional information about surface modified β -CD-NSP. The samples were placed into hermetically sealed aluminium pans and heated from 50 °C to 250 °C at a constant rate of 10 °C·min⁻¹. Analysis of the DSC thermal profiles was conducted using Mettler Toledo STAR software system. The obtained DSC data was used to detect the remaining crosslinking capacity and infer the degree of crosslinking by comparing it to overall crosslink capacity of pure β -CD (Brogly, Nardin, & Schultz, 1997; Hirschl et al., 2013; Stark & Jaunich,

2011). This degree of crosslinking (D_c) was determined from the enthalpy ΔH_t of β -CD-NSP in comparison to enthalpy ΔH_s of β -CD according to Formula (2)

$$D_c = \frac{\Delta H_s - \Delta H_t}{\Delta H_s} \quad (2)$$

Thermogravimetric analysis (TGA) was carried out in Perkin-Elmer Pyris-1 TGA equipment (USA), using dry air with a nitrogen gas flow of $20 \text{ mL}\cdot\text{min}^{-1}$ at the scan rate of $10^\circ\text{C}\cdot\text{min}^{-1}$. Samples were weighted (approximately 5 mg) in hanging aluminium pan and weight loss of samples monitored from 40°C to 600°C . Samples were analyzed with Star Pyris software. Further graphs were plotted by Origin Pro 8 software.

2.4.5. Crystallinity study

The crystallinity of the samples was characterized with Powder X ray diffraction (PXRD). Diffraction patterns of the β -CD-NSP-CHS samples were analyzed with a Bruker D8 advance diffractometer (Bruker, Germany) at ambient temperature, with the tube voltage of 40 kV and tube current of 40 mA in a stepwise scan mode ($8^\circ\cdot\text{min}^{-1}$). The samples were irradiated with monochromatized CuK α radiation and analyzed over a 2θ angle range of $3\text{--}40^\circ$. The obtained data were processed through the Origin Pro 8 software.

2.5. Quantification of CHS in surface modified NSP and phenol content determination

The CHS content in the β -CD-NSP samples was determined with a high-performance liquid chromatography (HPLC Agilent Technology, 1290 infinity, USA) with evaporative light scattering detector (ELSD, Model-Agilent Technology 1260 ELSD). The cholesterol succinate was recovered from the NSP sample by hydrolysis of ester bond using ammonia (NH_3). Briefly, about 30 mg of β -CD-NSP-CHS sample was dispersed in $800 \mu\text{L}$ of Milli-Q water and $200 \mu\text{L}$ ammonia (NH_3) solution. After 20 min sonication, the carbonyl bonds between CDs molecules as well as CD-CHS were degraded and hazy solution of suspended CHS obtained. Finally, 2 mL of methanol was added to dissolve the CHS in the diluent and centrifuged the solution at 12000 rpm for 5 mins to separate the soluble CHS. The supernatant layer was filtered through $0.22 \mu\text{m}$ membrane filter and injected into HPLC. In case of NSP, after hydrolysis with ammonia clear solution of CDs was obtained and diluted with water to detect the of β -CD peaks. The standard samples were prepared in the same way by using 3.0 mg of CHS reference standard. The details of HPLC method are listed in SI (supporting information).

Phenol was the main by-product of the reactions and it was very important to remove phenol completely for pharmaceutical applications. So, to determine the phenol content, NSP and CHS grafted NSP samples were hydrolysed by using ammonia same as for CHS content determination. A previously reported HPLC method was applied with slight modification (Gyorik, Herpai, Szecsenyi, Varga, & Szigeti, 2003) to detect the phenol concentration in the samples with a reference standard. The detail information about method and sample preparation is listed in SI.

2.6. Drug adsorption study

Dox was selected as a model drug to check the adsorption capacity and cellular uptake due to its fluorescence property which is suitable for cell experiments. The adsorption study was determined by supernatant layer method with validated HPLC method. Distilled water was used as a medium due to the good aqueous solubility of Dox. In the experiment, 500 mg of samples were incubated with 20 mL aqueous solution of Dox with total concentration of $2.5 \text{ mg}\cdot\text{mL}^{-1}$. After shaking (100 rpm) for 24 h at room temperature, the samples were withdrawn, centrifuged (4800 rpm), and the Dox amount was evaluated in the supernatant. The

drug adsorption formula and HPLC method used for Dox are listed in SI.

2.7. Drug release study

To check the drug release profiles of Dox, phosphate buffer pH 6.8 and pH 1.2 HCl buffer were used as release medium. Briefly, 10 mg Dox equivalent samples were placed into 100 mL of buffer solutions by using dissolution apparatus (Distek, USA) with USP apparatus-2 (paddle) at 37°C . At predetermined time intervals, 0.5 mL of released solution was taken out for testing and replenished with equivalent fresh buffer. The amount of Dox released form the NSP and CHS grafted NSP was determined by HPLC with UV detector at 233 nm. Each sample release study was conducted in triplicates.

2.7.1. In vitro cytotoxicity

The HeLa cells were obtained from cell bank of Chinese Academy of Sciences and further sub-cultured as per protocol reported in SI. In vitro cytotoxicity of surface modified NSPs samples was tested using the enhanced cell counting kit-8 (CCK-8, Beyotime). To determine the in vitro cytotoxicity, HeLa cells were seeded into 96-well plates and incubated for 24 h (5000 cells per well). The cells were treated with samples ($20 \mu\text{L}$) for 12 h. After that, CCK-8 solution ($10 \mu\text{L}$) was added to each well and incubated for 3 h. Every treatment was tested in eight individual wells. At the end of the experiment, the absorbance was measured at 450 nm using microplate reader (Thermo scientific, Multiscan Go, USA). The cell viability was calculated according to Formula (3),

$$\text{Cell Viability}(\%) = \frac{\text{OD}_{\text{exp}} - \text{OD}_{\text{blank}}}{\text{OD}_{\text{control}} - \text{OD}_{\text{blank}}} \times 100 \quad (3)$$

where OD_{exp} was absorbance of the sample, OD_{blank} was absorbance of blank, and $\text{OD}_{\text{control}}$ was absorbance of the control sample.

2.8. Cellular uptake study by laser scanning confocal microscopy

Cellular uptake study was carried out in order to investigate the effect on cellular uptake activity of surface modified β -CD-NSP on HeLa cells. To determine the cellular uptake, the HeLa cells were seeded onto glass bottom dishes at density of 1×10^4 cells per well and incubated at 37°C in a humidified chamber with 4% CO_2 for overnight. After incubation, the medium was replaced with fresh medium and β -CD-NSP-CHS and Dox control samples were added to each dish at a final concentration of $50 \text{ ng}\cdot\text{mL}^{-1}$. Cells were incubated for 6 h at 37°C . After incubation, cells were washed three times with phosphate buffer saline (PBS) and fixed with 0.5 mL of 4% paraformaldehyde for 10 mins at room temperature and treated with PBS. The nucleus was stained with DAPI H1200 for 5 min. Intracellular localization of Dox was recorded by CLSM (Leica microscopic system, Germany) and confocal images were processed by LAS-X software.

3. Results and discussion

3.1. Synthesis and surface modification of β -CD-NSP

In order to prepare β -CD-NSP and surface modification of nanosponges, a well-developed method was adopted which were previously reported from our lab. Free availability of hydroxyl group of β -CD makes it a suitable candidate for inter-crosslinking by the suitable electrophiles. The easily accessible crosslinking between hydroxyl groups was done via formation of carbonyl bond. A large number of crosslinkers was reported previously but we adopted DPC due to its high reactivity and easy availability. Specially, TEA acts as a nucleophile and opens up the carbonate ester of DPC and facilitates the proton exchange, which finally results in fast esterification of CD hydroxyl groups. After completion of the condensation polymerization reaction, gelation was observed. The selected electrophile is responsible for the

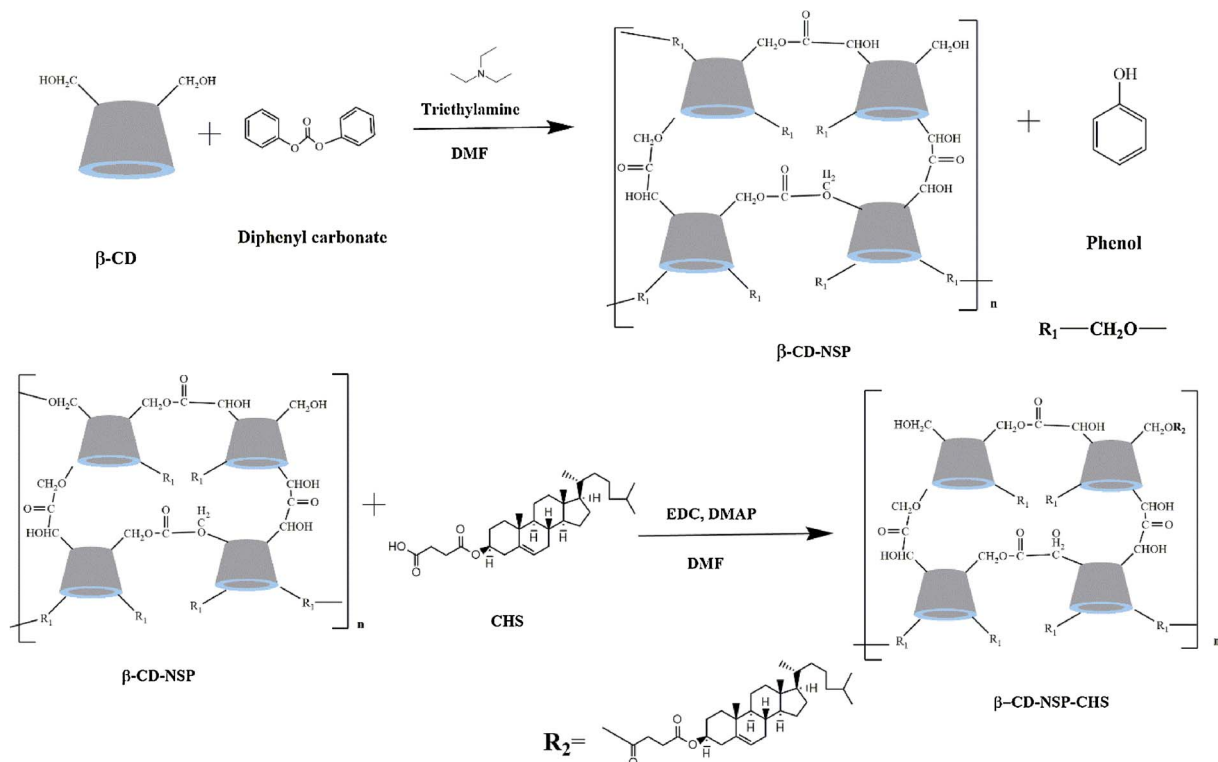


Fig. 1. Synthesis route of β -CD-NSP and CHS grafting by using coupling reaction.

formation of a bridge between two β -CD units (Fig. 1).

An optimized one-step chemical reaction was used for the surface modification of β -CD-NSP at 45 °C in DMF for 24 h. The unreacted cholesterol and catalysts were washed with water and ethanol. After lyophilization, samples were processed for further characterization.

3.2. SR-FTIR characterization

FTIR is a simple and frequently used technique by which organic molecule and their functional groups are characterized. FTIR spectra of β -CD-NSP (Fig. 2A) confirmed the successful synthesis of β -CD-NSP by chemical crosslinking between two β -CD molecules. As per previous

research, the characteristic peak of the carbonyl group (C=O) between the hydroxyl group of two β -CD molecules was observed at 1755 cm⁻¹, which confirmed the linkage of CDs via diphenyl carbonate (Singh, Xu et al., 2017).

The spectra of β -CD-NSP-CHS showed an intense signal around 3380 cm⁻¹ accounting for the presence of OH group in β -CD-NSP and CHS. The peak of C=O bond of anhydride at 1737 cm⁻¹ indicates the anhydride bond formation in β -CD-NSP and another peak was observed at 1757 cm⁻¹ showed the conjugated carbonyl ester peak of NSPs formation. The peak at 2868 cm⁻¹ medium appearance account for the presence of C–H stretching of CHS in β -CD-NSPs and at 1660 cm⁻¹ medium stretching account for carbonyl bond of β -CD.

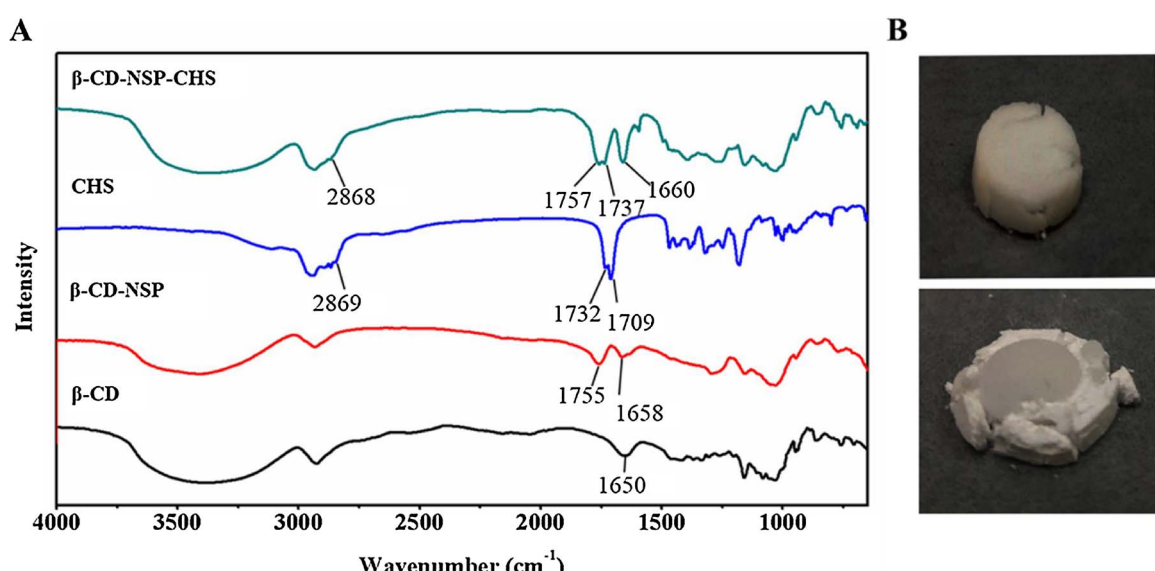


Fig. 2. SR-FTIR spectra of β -CD, β -CD-NSP, CHS, and β -CD-NSP-CHS for structural confirmation. The specific peak of successful crosslinking marked with wave numbers (A). Digital photograph of β -CD-NSP and β -CD-NSP-CHS after placing a drop of water on the tablet.

3.3. Water contact angle and swelling study

As a consequence, in water contact angle measurements, the β -CD-NSP acquired zero water contact angle due to the highly hydrophilic nature. The β -CD-NSP absorbed water drops within and swelled quickly. While a drop of water was placed onto the top surface of β -CD-NSP-CHS, the tablet showed hydrophobic nature by adopting half round shape. The water contact angle was measured manually as $93^\circ \pm 1$ by using Image Pro-Plus software as showing the hydrophobic nature of β -CD-NSP-CHS (Fig. 2B).

In water, β -CD-NSP showed swelling properties, which is mainly attributed to the high crosslinking between hydroxyl groups of β -CD. After grafting with CHS, the swelling property of NSP was significantly decreased due to hydrophobic nature and highly negative charge of CHS which prevent the crosslinked polymer from gelation. For CHS grafted NSP, the swelling ratio was recorded $0.03 \text{ mg}\cdot\text{mL}^{-1}$, which was very less compared to $0.08 \text{ mg}\cdot\text{mL}^{-1}$ of β -CD-NSP.

3.4. Zeta potential and particle size measurement

Particle size and zeta potential are important factors for determining the absorption of drug carrier and cellular penetration (Blanco, Shen, & Ferrari, 2015). The average zeta potential for β -CD-NSP and β -CD-NSP-CHS were recorded as $-5.03 \pm 2.00 \text{ mV}$, and $-18.0 \pm 2.00 \text{ mV}$ respectively (Fig. S-2). Therefore, hydrophobic nature of cholesterol increased the negative charge which could be useful for the stability of β -CD-NSP. The hydrophobic nature of grafted NSP prevents the molecules to interact with each other which changed the properties of NSP significantly. Moreover, the surface charge on the drug carriers plays important role in drug loading efficiency and can determine whether a charge active material will encapsulate in center of drug carrier or on the surface (Jung et al., 2001). The average particle size of β -CD-NSP-CHS was $390 \pm 20 \text{ nm}$ (Fig. S-2). The nanosize of NSP can penetrate into the cells, bind with nucleus membrane and release the drugs.

3.5. Thermal evaluation

All the samples were subjected to DSC and TGA for thermal properties evaluation. The thermal transition of β -CD-NSP can be explained by DSC graphs (Fig. 3A). In the presented graph, the thermal transition of NSP differs from the β -CD (In case of β -CD a sharp endothermic heat transitions peak was observed between 80 and 130°C while β -CD-NSP did not show any peak). The second relevant feature is endothermic, negative peak of crosslinking which was observed in the range $80\text{--}130^\circ\text{C}$. This peak was related to heat generation in crosslinking reaction which changed the enthalpy of the final products significantly. Furthermore, fitting reaction kinetics to experimentally determined data set showed the average DSC degree of crosslinking was $85 \pm 4\%$. Meanwhile, no exothermic, endothermic or crystallization behaviours were showed by β -CD-NSP-CHS. The DSC patterns of CHS showed crystallization peaks between 178 and 180°C . Moreover, the data also supported the amorphous nature of compounds which later confirmed by PXRD data.

TGA technique provides important information about the thermal stability of materials. In some cases, this technique has allowed us to achieve semi-quantitative information on composition (Riela et al., 2011). The TGA data of surface modified β -CD-NSP samples showed the behaviour according to a moiety attached onto the surface of β -CD-NSP (Fig. 3B). Another part of TGA is a residual analysis, which is an important piece of information about compound compositions. In the TGA experiment, the residue of CHS was 1.7% and for β -CD-NSP, it was 3.5% at 600°C respectively. However, the residue of CHS grafted sample remained 2.6% at 600°C showing the presence of CHS. Overall, data supported the successful surface modification of β -CD-NSP with CHS. The degradation and weight loss patterns are depicted in DTG curve (Fig. S-3).

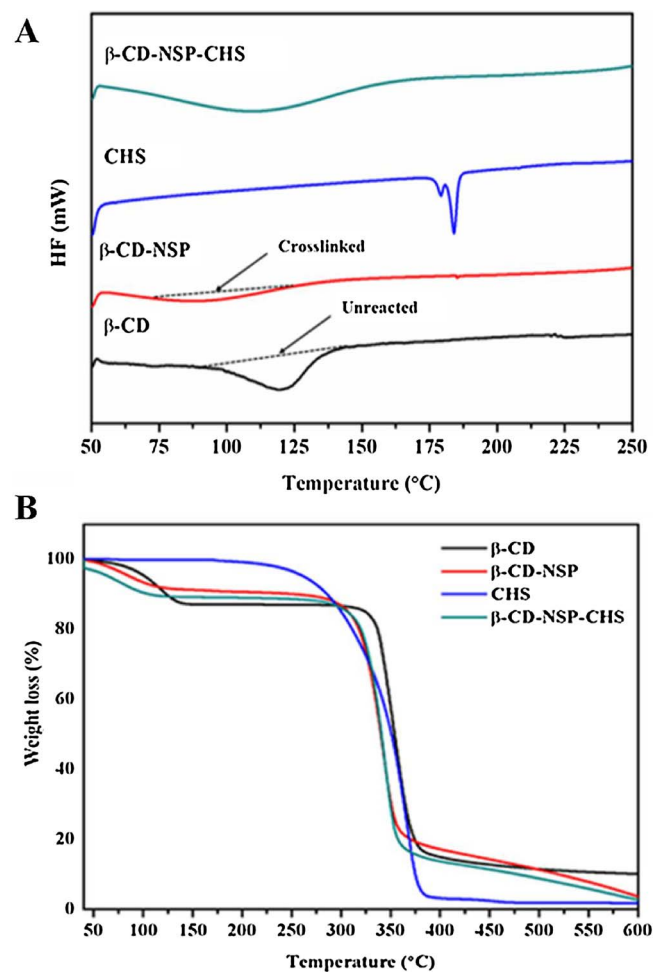


Fig. 3. DSC graphs of β -CD, β -CD-NSP, CHS, and β -CD-NSP-CHS showing no heat transition or crystallization point in surface modified NSP and β -CD-NSP (A). TGA graph of β -CD, β -CD-NSP, CHS, and β -CD-NSP-CHS (B) showing thermal degradation and remained residue in graph which supports the attachment of CHS over the surface of β -CD-NSP.

3.6. PXRD analysis of surface modified β -CD-NSP

The PXRD is a very useful technique to study the structural arrangement within the material. The structural arrangement of inside the molecule could interfere with drug encapsulation and drug release behaviours. Crystalline intense signals of β -CD were observed at 2θ of 4.7° , 9.1° , 10.7° , 11.8° , 14.9° , 17.2° , 19.8° and 23° , while crystal structure of β -CD was converted into amorphous due (Fig. 4) to the polymerization reaction which resembles with previously reported research (Mihailisa et al., 2016; Singh, Xu et al., 2017). The result was indicating that β -CD molecules distributed homogeneously in NSP without forming any phase-separated crystal aggregates. Interestingly, after grafting of crystalline CHS moiety onto amorphous β -CD-NSP, the amorphous nature was retained and no peaks were observed in PXRD analysis.

3.7. Quantification of CHS in surface modified NSP and phenol content determination

HPLC is most reliable and frequently used technique for quantification of compounds and able to detect trace numbers of other molecules present in samples. For quantification of CHS content in NSP, we developed a method based on ELSD detector (Fig. S-4). ELSD detector was selected due to its advantages of low baseline noise, accurate precision and suitability for detection of cyclodextrin and CHS (Lafosse, Elfakir, Morinallory, & Dreux, 1992). The calculated average content of

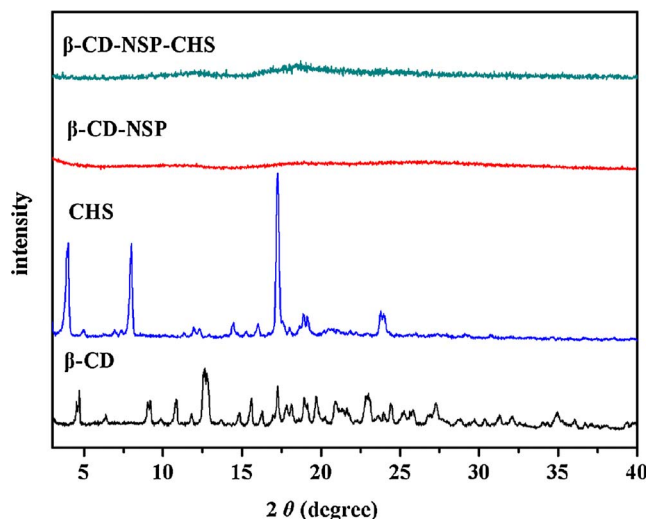


Fig. 4. PXRD graph of β -CD, β -CD-NSP, and β -CD-NSP-CHS. The PXRD pattern of surface modified β -CD-NSP shows the amorphous nature.

CHS was 1.51% (w/w) present in the β -CD-NSP (Fig. S-5). Nevertheless, the detected amount is proved enough to produce the effects in cellular experiments.

Moreover, to check the phenol content in the final product, carbonyl bond was hydrolysed by using ammonia to dissolve the phenol in diluent. Degraded samples were subjected to HPLC with UV detector to detect the amount of phenol. In contrast, the phenol peak was observed with negligible intensity (0.002% w/w). The obtained chromatograms are depicted in Fig. S-6.

3.8. Drug adsorption study

An adsorption study of Dox was carried out by supernatant layer method to check the drug adsorption efficiency of surface modified crosslinked polymer and concentration of Dox was determined by previously reported HPLC method (Singh et al., 2018). In our previous research, we optimized the Dox encapsulation efficiency with different degrees of crosslinking. The optimized crosslinked ratio was selected for

surface modification as well as drug adsorption efficiency (Singh, Xu et al., 2017). The drug adsorption capacity of β -CD-NSP-CHS was recorded 2.5% w/w which was 5.8% higher than β -CD-NSP (Fig. S-7). The hydrophobic nature of surface might be responsible for this enhancement of drug adsorption efficiency of NSP. To support the successful drug encapsulation within the surface modified β -CD-NSP, we performed the TGA analysis to check the changes in thermal behaviour as well as in residual mass (Fig. S-8). Interestingly, the residual mass of β -CD-NSP-CHS was increased significantly which support the presence of Dox in the β -CD-NSP-CHS. Similarly, DTG data also supported the Dox inclusion complex formation.

3.9. Drug release study

The Dox release profiles of β -CD-NSP-Dox and β -CD-NSP-CHS-Dox were analyzed by dissolution apparatus against buffer at pH 6.8 and pH 1.2. As shown in Fig. 5, the release profiles of both samples almost remained same which confirming CHS grafting did not change the release patterns of NSP. However, in phosphate buffer at 6.8 pH, CHS grafted NSP showed relatively fast release in starting while after 2 h the release profile became almost same. In addition, at pH 6.8 less than 30% Dox escaped from the NSP structure. However, NSP and CHS grafted NSP were showed high drug release profile at pH 1.2 and almost 82% drug diffused out within 15 mins. Later drug release profile showed almost similar patterns. The results were completely in agreement with previously reported research (Huang, Zhu, Wang, Mo, & Hua, 2017).

3.10. In vitro cytotoxicity

The cytotoxicity of surface modified β -CD-NSP was determined in cervical cancer cell line (HeLa cell) and obtained data are presented in Fig. 6. The data showed surface modified β -CD-NSP samples were biofriendly and did not exert any significant toxicity in HeLa cells. The viability of HeLa cells was not much affected even at high concentration of samples up to $100 \mu\text{g}\cdot\text{mL}^{-1}$. The modified β -CD-NSP was biocompatible and found safe for drug delivery applications.

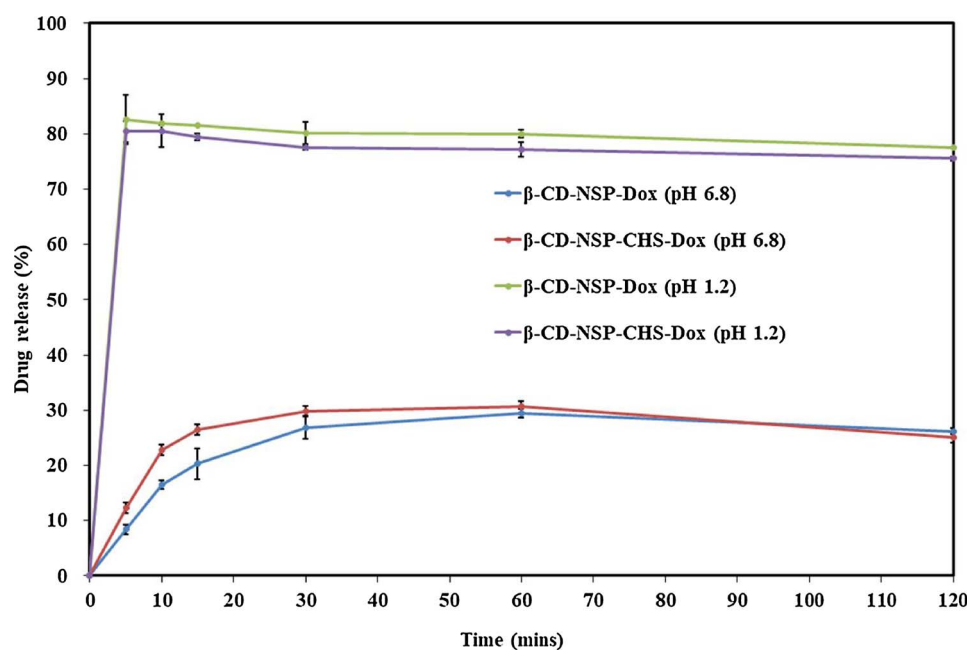


Fig. 5. Drug release profiles of β -CD-NSP-Dox and β -CD-NSP-CHS-Dox at pH 6.8 (phosphate buffer) and pH 1.2 HCl solution. The data were expressed as mean \pm SDs ($n = 3$).

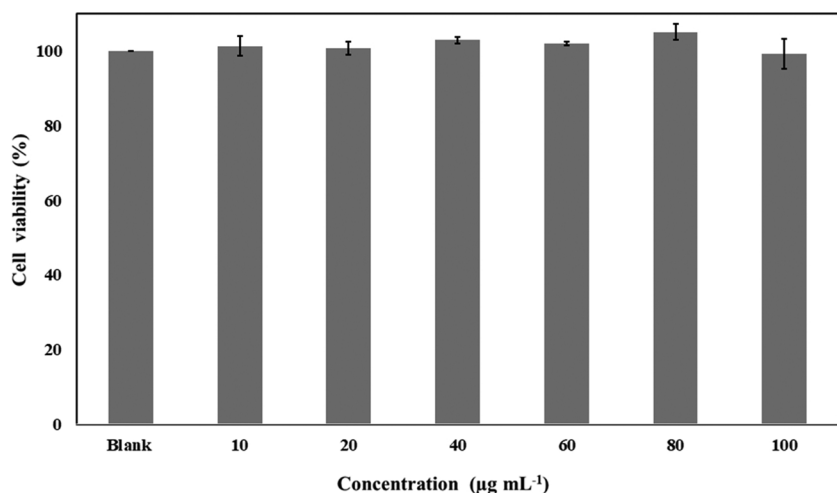


Fig. 6. Cell viability assay graph of β -CD-NSP-CHS in HeLa cells shows no cytotoxic effect over 12 h incubation at different concentrations.

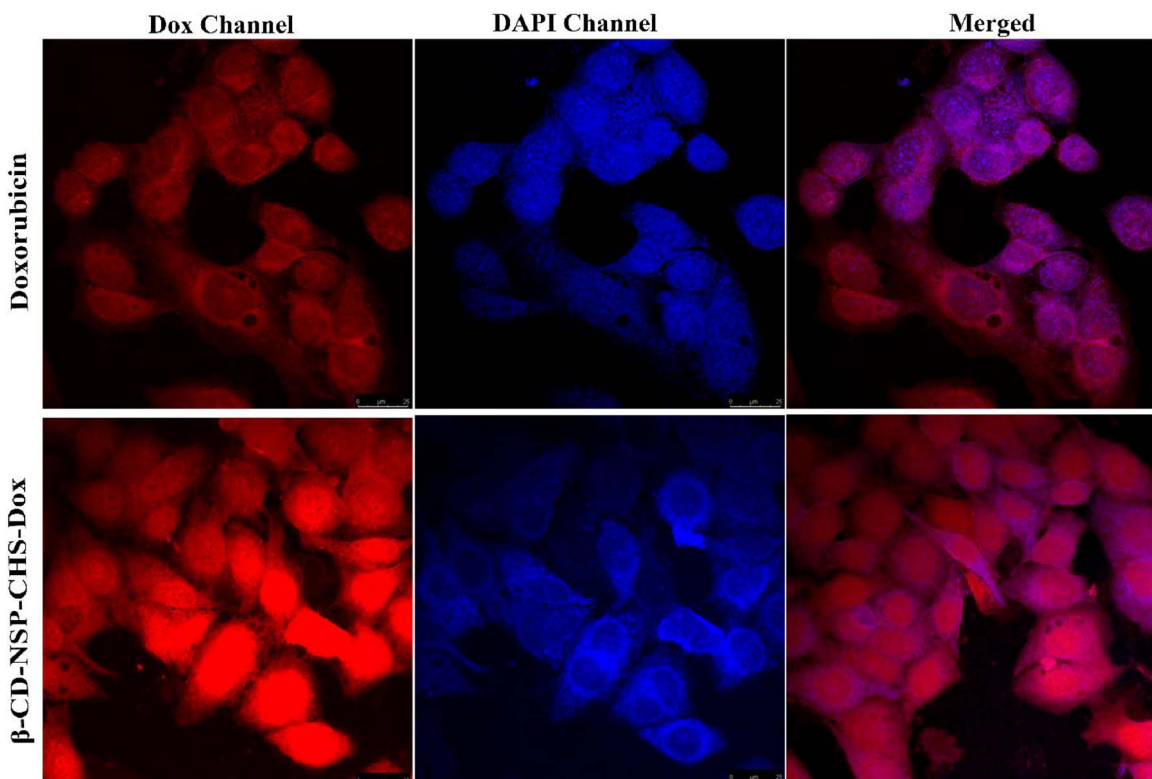


Fig. 7. The confocal images showing cellular uptake of Dox loaded β -CD NSP-CHS and free Dox in comparison. The merged channel of β -CD-NSP-CHS shows the accumulation of the drug around nucleus membrane. The images were representative of three experiments with similar results.

3.11. Cellular uptake study by laser scanning confocal microscopy

It is well reported that CHS modification of nanoparticles can enhance the cellular uptake of Dox (Tang et al., 2014; Wang et al., 2016; Zhang et al., 2016). The phospholipid bilayer of nuclear membrane attracts CHS moiety containing the drug to bind onto the outer surface of the nucleus which leads to enhance cellular uptake. Dox loaded CHS surface modified β -CD-NSP was detected in HeLa cancer cell line using CLSM. The intracellular uptake of free Dox was compared with surface modified β -CD-NSP in HeLa cells and obtained results are represented in Fig. 7. For the experiment, HeLa cells were stained with DAPI to locate the nucleus and incubated for 6 h with free Dox and Dox loaded β -CD-NSP-CHS samples. The microscopic images were showed the higher intensity of drug accumulation inside or on the surface of the cell

nucleus as compare to free Dox which supports the CHS modification could enhance the drug penetration. This might be due to CHS role in enhancing cell internalization of the drug as previously reported (Chen et al., 2013).

4. Conclusions

In conclusion, the β -CD-NSP has been successfully synthesized and surface biofunctionalized with CHS for improvement in the therapeutic and drug delivery efficacy of CD-NSP. The CHS expression on CD-NSP has been confirmed by various spectroscopic and thermal analytical techniques. The CHS modification has changed the surface properties of β -CD-NSP in many ways. The results have demonstrated that CHS grafting can enhance the Dox adsorption because of hydrophobic

charge on the surface. In addition, the biofriendly nature of surface modified CD-NSP was verified with cell viability assay. The cellular uptake of the Dox loaded β -CD-NSP showed better internalization in cells due to the interaction between CHS and cell membrane. It is very much of interest that surface engineered CD-NSP could be used as a carrier for low water-soluble small drug molecules to improve the solubility and bioavailability in site specific drug delivery systems.

Acknowledgements

The authors are grateful for the financial support from the National Natural Science Foundation of China (No. 81430087) and National Science and Technology Major Project (2017ZX09101001-006). We gratefully acknowledge the staff from BL01B beamline of National Facility for Protein Science Shanghai (NFPS) at Shanghai Synchrotron Radiation Facility Center, for assistance during data collection. We thank the CAS-TWAS Presidential Fellowship Program for providing Ph.D. fellowship to the first author.

Appendix A. Supplementary data

Supplementary data associated with this article can be found, in the online version, at <https://doi.org/10.1016/j.carbpol.2018.02.044>.

References

Alongi, J., Poskovic, M., Frache, A., & Trotta, F. (2010). Novel flame retardants containing cyclodextrin nanosplices and phosphorus compounds to enhance EVA combustion properties. *Polymer Degradation and Stability*, 95(10), 2093–2100.

Ansari, K. A., Torne, S. J., Vavia, P. R., Trotta, F., & Cavalli, R. (2011). Paclitaxel loaded nanosplices: In-vitro characterization and cytotoxicity study on MCF-7 cell line culture. *Current Drug Delivery*, 8(2), 194–202.

Blanco, E., Shen, H., & Ferrari, M. (2015). Principles of nanoparticle design for overcoming biological barriers to drug delivery. *Nature Biotechnology*, 33(9), 941–951.

Brogly, M., Nardin, M., & Schultz, J. (1997). Effect of vinylacetate content on crystallinity and second-order transitions in ethylene–Vinylacetate copolymers. *Journal of Applied Polymer Science*, 64(10), 1903–1912.

Caldera, F., Tannous, M., Cavalli, R., Zanetti, M., & Trotta, F. (2017). Evolution of cyclodextrin nanosplices. *International Journal of Pharmaceutics*, 531(2), 470–479.

Chen, C.-J., Wang, J.-C., Zhao, E.-Y., Gao, L.-Y., Feng, Q., Liu, X.-Y., & Zhang, Q. (2013). Self-assembly cationic nanoparticles based on cholesterol-grafted bioreducible poly (amidoamine) for siRNA delivery. *Biomaterials*, 34(21), 5303–5316.

Chilajwar, S. V., Pednekar, P. P., Jadhav, K. R., Gupta, G. J. C., & Kadam, V. J. (2014). Cyclodextrin-based nanosplices: A propitious platform for enhancing drug delivery. *Expert Opinion on Drug Delivery*, 11(1), 111–120.

Crini, G. (2014). Review: A history of cyclodextrins. *Chemical Reviews*, 114(21), 10940–10975.

Ercole, F., Whittaker, M. R., Quinn, J. F., & Davis, T. P. (2015). Cholesterol modified self-assemblies and their application to nanomedicine. *Biomacromolecules*, 16(7), 1886–1914.

Gigliotti, C. L., Minelli, R., Cavalli, R., Occhipinti, S., Barrera, G., Pizzimenti, S., & Dianzani, C. (2016). In vitro and in vivo therapeutic evaluation of camptothecin-encapsulated beta-cyclodextrin nanosplices in prostate cancer. *Journal of Biomedical Nanotechnology*, 12(1), 114–127.

Guo, Z., Wu, F., Singh, V., Guo, T., Ren, X., Yin, X., & Zhang, J. (2017). Host-guest kinetic interactions between HP- β -cyclodextrin and drugs for prediction of bitter taste masking. *Journal of Pharmaceutical and Biomedical Analysis*, 140(Suppl. C), 232–238.

Gyorik, M., Herpai, Z., Szecsenyi, I., Varga, L., & Szegedi, J. (2003). Rapid and sensitive determination of phenol in honey by high-performance liquid chromatography with fluorescence detection. *Journal of Agricultural and Food Chemistry*, 51(18), 5222–5225.

Hartlieb, K. J., Holcroft, J. M., Moghadam, P. Z., Vermeulen, N. A., Algaradah, M. M., Nassar, M. S., & Stoddart, J. F. (2016). CD-MOF: A versatile separation medium. *Journal of the American Chemical Society*, 138(7), 2292–2301.

Hirsch, C., Biebl-Rydlo, M., DeBiasio, M., Mühleisen, W., Neumaier, L., Scherf, W., & Kraft, M. (2013). Determining the degree of crosslinking of ethylene vinyl acetate photovoltaic module encapsulants—A comparative study. *Solar Energy Materials and Solar Cells*, 116, 203–218.

Hosta-Rigau, L., Zhang, Y., Teo, B. M., Postma, A., & Stadler, B. (2013). Cholesterol – A biological compound as a building block in bionanotechnology. *Nanoscale*, 5(1), 89–109.

Huang, K., Zhu, L., Wang, Y., Mo, R., & Hua, Z. (2017). Targeted delivery and release of doxorubicin using a pH-responsive and self-assembling copolymer. *Journal of Materials Chemistry B*, 5(31), 6356–6365.

Ikonen, E. (2008). Cellular cholesterol trafficking and compartmentalization. *Nature Reviews Molecular Cell Biology*, 9(2), 125–138.

Jung, T., Kamm, W., Breitenbach, A., Hungerer, K. D., Hundt, E., & Kissel, T. (2001). Tetanus toxoid loaded nanoparticles from sulfobutylated poly(vinyl alcohol)-graft-poly(lactide-co-glycolide): Evaluation of antibody response after oral and nasal application in mice. *Pharmaceutical Research*, 18(3), 352–360.

Lafosse, M., Elfakir, C., Morinallory, L., & Dreux, M. (1992). The advantages of evaporative light-scattering detection in pharmaceutical analysis by high-performance liquid-chromatography and supercritical fluid chromatography. *HRC – Journal of High Resolution Chromatography*, 15(5), 312–318.

Loftsson, T., Brewster, M. E., & Måsson, M. (2004). Role of cyclodextrins in improving oral drug delivery. *American Journal of Drug Delivery*, 2(4), 261–275.

Ma, X., & Zhao, Y. (2015). Biomedical applications of supramolecular systems based on host-guest interactions. *Chemical Reviews*, 115(15), 7794–7839.

Mejia-Ariza, R., Grana-Suarez, L., Verboom, W., & Huskens, J. (2017). Cyclodextrin-based supramolecular nanoparticles for biomedical applications. *Journal of Materials Chemistry B*, 5(1), 36–52.

Mihailaia, M., Caldera, F., Li, J., Peila, R., Ferri, A., & Trotta, F. (2016). Preparation of functionalized cotton fabrics by means of melatonin loaded beta-cyclodextrin nanosplices. *Carbohydrate Polymers*, 142, 24–30.

Murata, M., Peranen, J., Schreiner, R., Wieland, F., Kurzhalia, T. V., & Simons, K. (1995). VIP21/caveolin is a cholesterol-binding protein. *Proceedings of the National Academy of Sciences of the United States of America*, 92(22), 10339–10343.

Nohturfft, A., Brown, M. S., & Goldstein, J. L. (1998). Sterols regulate processing of carbohydrate chains of wild-type SREBP cleavage-activating protein (SCAP), but not sterol-resistant mutants Y298C or D443N. *Proceedings of the National Academy of Sciences*, 95(22), 12848–12853.

Park, J., Brust, T. F., Lee, H. J., Lee, S. C., Watts, V. J., & Yeo, Y. (2014). Polydopamine-based simple and versatile surface modification of polymeric nano drug carriers. *ACS Nano*, 8(4), 3347–3356.

Riela, S., Lazzara, G., Lo Meo, P., Guernelli, S., D'Anna, F., Milioti, S., & Noto, R. (2011). Microwave-assisted synthesis of novel cyclodextrin-cucurbituril complexes. *Supramolecular Chemistry*, 23(12), 819–828.

Shen, S., Li, H., & Yang, W. (2014). The preliminary evaluation on cholesterol-modified pullulan as a drug nanocarrier. *Drug Delivery*, 21(7), 501–508.

Sherje, A. P., Dravyakar, B. R., Kadam, D., & Jadhav, M. (2017). Cyclodextrin-based nanosplices: A critical review. *Carbohydrate Polymers*, 173, 37–49.

Simons, K., & Vaz, W. L. (2004). Model systems, lipid rafts, and cell membranes. *Annual Review of Biophysics and Biomolecular Structure*, 33, 269–295.

Singh, P., Ren, X., He, Y., Wu, L., Wang, C., Li, H., & Zhang, J. (2018). Fabrication of β -cyclodextrin and sialic acid copolymer by single pot reaction to site specific drug delivery. *Arabian Journal of Chemistry*. <http://dx.doi.org/10.1016/j.arabjc.2017.11.011>.

Singh, V., Guo, T., Xu, H., Wu, L., Gu, J., Wu, C., & Zhang, J. (2017). Moisture resistant and biofriendly CD-MOF nanoparticles obtained via cholesterol shielding. *Chemical Communications*, 53(66), 9246–9249.

Singh, V., Xu, J., Wu, L., Liu, B., Guo, Z., & Zhang, J. (2017). Ordered and disordered cyclodextrin nanosplices with diverse physicochemical properties. *RSC Advances*, 7(38), 23759–23764.

Stark, W., & Jaunich, M. (2011). Investigation of ethylene/vinyl acetate copolymer (EVA) by thermal analysis DSC and DMA. *Polymer Testing*, 30(2), 236–242.

Swaminathan, S., Pastero, L., Serpe, L., Trotta, F., Vavia, P., Aquilano, D., & Cavalli, R. (2010). Cyclodextrin-based nanosplices encapsulating camptothecin: Physicochemical characterization, stability and cytotoxicity. *European Journal of Pharmaceutics and Biopharmaceutics*, 74(2), 193–201.

Swaminathan, S., Cavalli, R., & Trotta, F. (2016). Cyclodextrin-based nanosplices: A versatile platform for cancer nanotherapeutics development. *Wiley Interdiscip Rev Nanomed Nanobiotechnol*, 8(4), 579–601.

Szejtli, J. (1998). Introduction and general overview of cyclodextrin chemistry. *Chemical Reviews*, 98(5), 1743–1754.

Tang, J., Fu, H., Kuang, Q. F., Zhang, Q. Y., Liu, Y. Y., & He, Q. (2014). Liposomes co-modified with cholesterol anchored cleavable PEG and octaarginines for tumor targeted drug delivery. *Journal of Drug Targeting*, 22(4), 313–326.

Trotta, F., Caldera, F., Dianzani, C., Argenziano, M., Barrera, G., & Cavalli, R. (2016). Glutathione bioresponsive cyclodextrin nanosplices. *ChemPlusChem*, 81(5), 439–443.

Venuti, V., Rossi, B., Mele, A., Melone, L., Punta, C., Majolino, D., & Trotta, F. (2017). Tuning structural parameters for the optimization of drug delivery performance of cyclodextrin-based nanosplices. *Expert Opinion on Drug Delivery*, 14(3), 331–340.

Wang, H. Y., Hua, X. W., Jia, H. R., Liu, P. D., Gu, N., Chen, Z., & Wu, F. G. (2016). Enhanced cell membrane enrichment and subsequent cellular internalization of quantum dots via cell surface engineering: Illuminating plasma membranes with quantum dots. *Journal of Materials Chemistry B*, 4(5), 834–843.

Wang, Y., Liu, Y., Liang, J., & Zou, M. (2017). A cyclodextrin-core star copolymer with Y-shaped ABC miktoarms and its unimolecular micelles. *RSC Advances*, 7(19), 11691–11700.

Zhang, J. X., & Ma, P. X. (2013). Cyclodextrin-based supramolecular systems for drug delivery: Recent progress and future perspective. *Advanced Drug Delivery Reviews*, 65(9), 1215–1233.

Zhang, L., Bennett, W. F. D., Zheng, T., Ouyang, P. K., Ouyang, X. P., Qiu, X. Q., & Chen, P. (2016). Effect of cholesterol on cellular uptake of cancer drugs pirarubicin and ellipticine. *Journal of Physical Chemistry B*, 120(12), 3148–3156.